

Identifying the Membrane Proteome of HIV-1 Latently Infected Cells^{*S}

Received for publication, July 3, 2006, and in revised form, January 18, 2007. Published, JBC Papers in Press, January 19, 2007, DOI 10.1074/jbc.M606324200

Reem Berro[‡], Cynthia de la Fuente^{§1}, Zachary Klase[¶], Kylee Kehn^{§2}, Lida Parvin^{||}, Anne Pumfery^{§3}, Emmanuel Agbottah[§], Akos Vertes^{||}, Sergei Nekhai^{**}, and Fatah Kashanchi^{‡§††4}

From the [‡]Genetics Program, [§]Department of Biochemistry and Molecular Biology, [¶]Department of Immunology, and ^{||}Department of Chemistry, The George Washington University, School of Medicine, Washington, D. C. 20037, ^{**}Department of Biochemistry/Center for Sickle Cell Disease, Howard University, Washington, D. C. 20059, and ^{††}The Institute for Genomic Research, Rockville, Maryland 20850

Profiling integral plasma membrane proteins is of particular importance for the identification of new biomarkers for diagnosis and for drug development. We report in this study the identification of surface markers by performing comparative proteomics of established human immunodeficiency virus-1 (HIV-1) latent cell models and parental cell lines. To this end we isolated integral membrane proteins using a biotin-directed affinity purification method. Isolated proteins were separated by two-dimensional gel electrophoresis and identified by matrix-assisted laser desorption/ionization-time-of-flight (MALDI-TOF) after in gel digestion. Seventeen different proteins were found to vary on the surface of T-cells due to HIV-1 infection. Of these proteins, 47% were integral membrane proteins, and 18% were membrane-associated. Through the use of complementary techniques such as Western blotting and fluorescent staining, we confirmed the differential expression of some of the proteins identified by MALDI-TOF including Bruton's tyrosine kinase and X-linked inhibitor of apoptosis. Finally, using phosphatidylinositol 3-kinase inhibitors and flavopiridol to inhibit Bruton's tyrosine kinase localization at the membrane and X-linked inhibitor of apoptosis protein expression, respectively, we showed that HIV-1 latently infected cells are more sensitive to these drugs than uninfected cells. This suggests that HIV-1 latently infected cells may be targeted with drugs that alter several pathways that are essential for the establishment and maintenance of latency.

Biological membranes surround and compartmentalize cells. They provide a physical boundary between the cell and its envi-

ronment and play an important role in cellular homeostasis and metabolic energy transduction. According to the Singer-Nicolson "fluid-mosaic model" (1), plasma membranes are organized into lipid bilayers containing proteins that can diffuse rapidly throughout the two-dimensional surface of the membrane. Membrane proteins typically make up around a third of the proteome of a cell and associate with the membrane in different ways. Integral membrane proteins are contained within the bilayer through one or more transmembrane regions. They can also be associated with lipid anchors such as fatty acids and can cover large regions of a membrane with protein surfaces. Alternatively, proteins can be associated with the membrane through non-covalent interactions with integral membrane proteins or other membrane-associated proteins. The fluidity differences and the organization of protein and lipids within the plasma membrane depend upon the cholesterol content in the bilayer (2). The current evidence supports a novel concept of specific microdomains existing in the plasma membrane *in vivo* in regions rich in cholesterol (2, 3). These specific microdomains, termed "lipid rafts," are composed of tightly packed sphingolipids, gangliosides, and cholesterol (4). Lipid rafts are generally small, ranging from 25 to 700 nm depending on the activation state of the cell (5). In addition to their small size, lipid rafts are mobile, enabling them to operate as floating devices that can transport specific proteins involved in many cellular processes (6, 7).

HIV⁵ infects several cell types during the course of infection and progression to acquired immune deficiency syndrome (AIDS). The virus establishes a persistent infection in CD4⁺ T lymphocytes and, to a lesser extent, macrophages, while creating a persistent reservoir mainly consisting of latently infected resting memory CD4⁺ T cells (8). Current therapies directed against viral proteins, highly active anti-retroviral therapy, have been problematic because of long-term toxicity, inhibitor resistance, and the inability to target persistent reservoirs. Thus, there is a need for new approaches to selectively target latent reservoirs and to discover unique protein targets for the design of therapeutic drugs.

* This work was supported by grants from the George Washington University REF funds (to R. B., F. K., and A. V.), a Snyder award, and National Institutes of Health Grants AI065236 and AI043894 (to F. K.). The costs of publication of this article were defrayed in part by the payment of page charges. This article must therefore be hereby marked "advertisement" in accordance with 18 U.S.C. Section 1734 solely to indicate this fact.

^S The on-line version of this article (available at <http://www.jbc.org>) contains supplemental Table 1.

¹ Current address: Laboratory of Virology and Infectious Disease, Center for the Study of Hepatitis C, The Rockefeller University, New York, NY 10021.

² Current address: Counterterrorism and Forensic Science Research Unit, Federal Bureau of Investigation Laboratory, Quantico, VA 22135.

³ Current address: Dept. of Biology, Seton Hall University, South Orange, NJ 07079.

⁴ To whom correspondence should be addressed: The George Washington University, 2300 I St., NW, Ross Hall, Rm. 551, Washington, D. C. 20037. Tel.: 202-994-1781; Fax: 202-994-1780; E-mail: bcmfxx@gwumc.edu.

⁵ The abbreviations used are: HIV, human immunodeficiency virus; BTK, Bruton's tyrosine kinase; XIAP, X-linked inhibitor of apoptosis; PMF, plasma membrane fractions; MALDI-TOF, matrix-assisted laser desorption/ionization-time-of-flight; PBMC, peripheral blood mononuclear cells; PBS, phosphate-buffered saline; PNS, post-nuclear supernatant; PARP, poly(ADP-ribose) polymerase; CHAPS, 3-[(3-cholamidopropyl)dimethylammonio]-1-propanesulfonic acid; FACS, fluorescence-activated cell sorting; GFP, green fluorescent protein; NaB, sodium butyrate; PI3K, phosphatidylinositol 3-kinase.

Membrane Proteome of HIV-1 Latently Infected Cells

Proteomics is a promising approach for the study of viruses. It allows a better understanding of pathogenesis and the development of new biomarkers for diagnosis and early detection of disease and accelerates drug development. However, most viral proteomics research has focused on determining the virion proteome or on identifying unique protein signatures from extracts of HIV-infected cells. Fuchigami *et al.* (10) identified 25 proteins within HIV-1 (LAV-1) virions by separating the proteins from purified HIV-1 particles by two-dimensional gel electrophoresis and identifying them by MALDI-TOF (9). In another study Carlson *et al.* (11) used a ProteinChip and surface enhancement laser desorption ionization to identify unique protein signatures in HIV-infected monocytes obtained from different donors. Although several thousand proteins were identified, they were all abundant cellular proteins (11). To reduce the complexity of this analysis, it is desirable to apply proteomics for the characterization of subcellular proteomes such as secreted proteins, surface proteins, and immunogenic proteins.

Our objective in this study was to identify surface markers on HIV-1 latently infected cells by performing comparative proteomics on established cell models of HIV-1 latency and parental cell lines. ACH2 cells are HIV-1 latently infected lymphocytic CEM (12D7) cells with a single integrated wild type provirus (12). They express only basal levels of viral mRNAs and proteins and do not produce high titer infectious virus without stimulation (13). We isolated integral membrane proteins by biotinylation and affinity purification as previously described (14), separated the isolated proteins by two-dimensional gel electrophoresis, and determined their identity by MALDI-TOF. Comparison of uninfected and latently infected cells allowed the identification of 17 differentially expressed proteins, on the cell surface of which 47% were found to be integral membrane proteins and 18% were membrane-associated, whereas 35% were either cytoplasmic- or organelle-associated. Many of these proteins belong to the receptor signaling, cell adhesion, and cytoskeleton pathways, and a few proteins were T-cell-specific including T cell receptor and junction adhesion molecule 3. Finally, we confirmed the differential expression in HIV latently infected cells of two proteins, BTK and XIAP, by immunoblotting and confocal microscopy and used specific inhibitors wortmannin, to inhibit BTK localization at the membrane, and flavopiridol, to inhibit XIAP protein expression. Furthermore, we showed that HIV-1 latently infected cells are more sensitive to these drugs than uninfected cells. Therefore, by comparing surface proteins of infected and uninfected cells, we have identified several pathways that are important for the maintenance of latency including cell survival and anti-apoptotic and cell adhesion/migration pathways. Targeting several of these pathways in infected cells may help define new therapies to eradicate latently infected cells that persist after highly active anti-retroviral therapy treatment.

EXPERIMENTAL PROCEDURES

Cell Lines, Peripheral Blood Mononuclear Cells (PBMC), and Plasmids

ACH2 (AIDS Research and Reference Reagents Program, National Institutes of Health) is an HIV-1-infected latent T-cell

clone derived from the parental CEM (A3.01) cells that were initially infected with the LAV strain of HIV-1. CEM (12D7) is an uninfected human T lymphoblastoid cell line, and A3.01 is a hypoxanthine/aminopterin/thymidine (HAT)-sensitive derivative of CEM. ACH2, A3.01, and CEM cells were cultured in RPMI 1640 containing 10% fetal bovine serum, 1% penicillin/streptomycin, and 1% L-glutamine (Quality Biological). HLM-1 cells (AIDS Research and Reference Reagents Program, NIH) are HeLa-T4+ cells containing one integrated copy of HIV-1 genome with a Tat-defective mutation at the first AUG of Tat gene. In the absence of stimulation, HLM-1 is completely negative for virus particle production, and viral transcripts are completely absent (15). HLM-1 and HeLa-T4+ were maintained in Dulbecco's modified Eagle's medium supplemented with 10% fetal bovine serum, 1% glutamine, and 1% penicillin/streptomycin (Quality Biological) and G418 (200 $\mu\text{g}/\text{ml}$) for selection. PBMC were isolated from healthy donor blood according to standard procedures. In brief, 10 ml of blood was layered over 5 ml of Ficoll and spun at $1000 \times g$ for 30 min with no braking. The white cell layer was removed and washed twice with PBS. Isolated PBMC were counted and resuspended in Dulbecco's modified Eagle's medium with 20% fetal bovine serum and 10% Me₂SO for storage in liquid nitrogen. PBMC were activated with phytohemagglutinin (5 $\mu\text{g}/\text{ml}$) in the presence of interleukin-2 (20 IU/ μl) and infected with HIV-1 LAI strain at 1000 TC50. The BTK-GFP plasmid was kindly provided by Dr. Smith (Huddinge University Hospital, Sweden) and previously described (16).

Plasma Membrane Protein Isolation

ACH2 and CEM (5×10^8 cells/isolation) were surface-biotinylated for 30 min at 4 °C using EZ-Link Sulfo-NHS-Biotin (Pierce), as previously described (14, 17). Cells were then centrifuged and washed twice with cold Dulbecco's PBS without Ca²⁺/Mg²⁺ to remove excess biotin. Next, cells were homogenized in ice-cold hypotonic buffer (10 mM HEPES, pH 7.5, 1.5 mM MgCl₂, 10 mM KCl, protease inhibitor mixture tablet, 1 mM NaF, and 1 mM Na₃VO₄) using a Dounce homogenizer (50 strokes). Lysates were centrifuged twice, first at $1000 \times g$ (10 min, 4 °C) to remove unbroken cells and nuclei (post-nuclear supernatant (PNS)) and then at $20,000 \times g$ (30 min, 4 °C) to precipitate plasma membrane and organelles. The PNS pellet was then resuspended in hypotonic buffer supplemented with 0.05% Triton X-100 and 150 mM KCl. Streptavidin-Sepharose beads were added to the PNS fraction and mixed overnight at 4 °C. Streptavidin complexes were precipitated by centrifugation and repeatedly washed twice with 1 M KCl, twice with 0.1 M Na₂CO₃, pH 11.5, and once with ice-cold hypotonic buffer to isolate integral membrane proteins. Proteins were subsequently precipitated with a mixture of trichloroacetic acid/acetone to allow for removal of lipids. The proteins were further concentrated by the addition of 20% trichloroacetic acid and incubation on dry ice for 30 min. The proteins were collected by centrifugation at $20,000 \times g$ for 10 min at 4 °C, washed with cold acetone, and finally solubilized in urea solubilization buffer (7 M urea, 2 M thiourea, 1% Triton X-100, 100 mM dithiothreitol, and protease inhibitors).

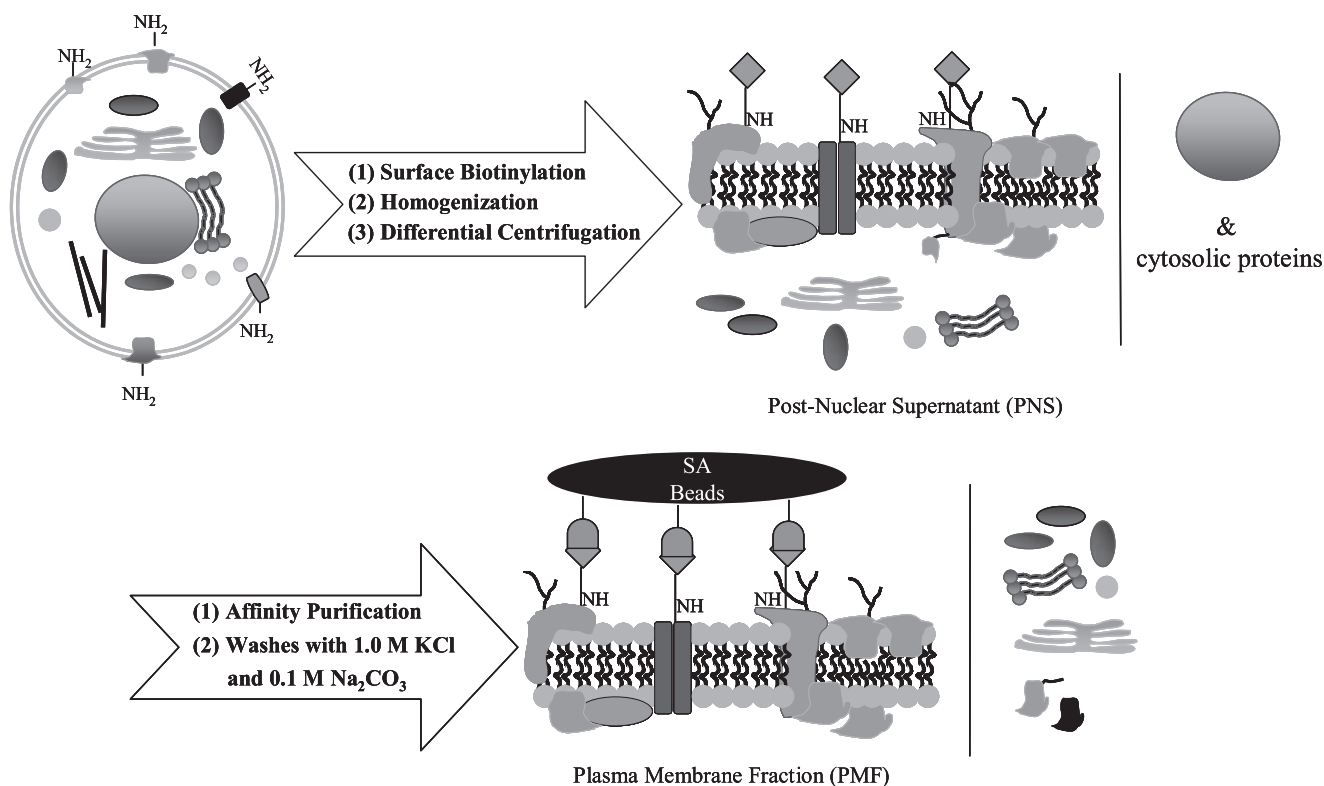


FIGURE 1. **Overview of plasma membrane protein isolation.** HIV-1-infected cells (ACH2) and uninfected parental cells (CEM) were surface-biotinylated, homogenized, and centrifuged to separate the nucleus and cytosolic proteins from the PNS. The PNS pellet was resuspended in hypotonic buffer, and streptavidin-Sepharose (SA) beads were added. PMFs were obtained after precipitation and washing of the beaded complexes to separate them from the cellular organelles.

Electrophoresis and Western Blot

One-dimensional SDS-PAGE—SDS-PAGE was carried out as described (18) with pre-cast gradient gels (4–20% Tris-glycine; Invitrogen). After electrophoresis, gels were either stained with Coomassie Blue R-250 or silver-stained using the SilverQuest kit (Invitrogen) or were transferred to a polyvinylidene difluoride membrane for Western blot analysis. BTK (611116) and XIAP (610762) antibodies were purchased from BD Biosciences, GRP94 (SPA-850) was from Stressgen, and Fas (C-20), PARP (H-250), caspase-3 (H-277), Mcl-1 (S-19), and actin (C-11) were from Santa Cruz Biotechnology.

Two-dimensional Gel Electrophoresis (Isoelectric Focusing/SDS-PAGE)—ACH2 (HIV+) and CEM (HIV-) plasma membrane fractions (PMF) in urea solubilization buffer were supplemented further with two-dimensional gel electrophoresis sample rehydration buffer (7 M urea, 2% CHAPS, 50 mM dithiothreitol, 0.2% (w/v) BioLyte 3/10 ampholytes, and bromphenol blue (trace)) (Bio-Rad). Processed samples from 5×10^8 cell equivalents were loaded onto an 11-cm pH 3–10 immobilized pH gradient strip through passive rehydration (16 h, room temperature). PMF proteins were focused for a total of 35,000 Vh (15 min at 250-V linear mode, 8000 V for 2:30-h linear mode and 8000 V to 25,000 Vh in rapid mode). Equilibration of immobilized pH gradient strips and two-dimensional gel electrophoresis were performed according to the manufacturer's recommendations (Bio-Rad) on a 4–20% Tris-glycine gel. Gels were stained with mass spectrometry-compatible silver stain (Invitrogen). Imaging of gels was performed using the Bio-Rad FluorS imager. Numbered spots

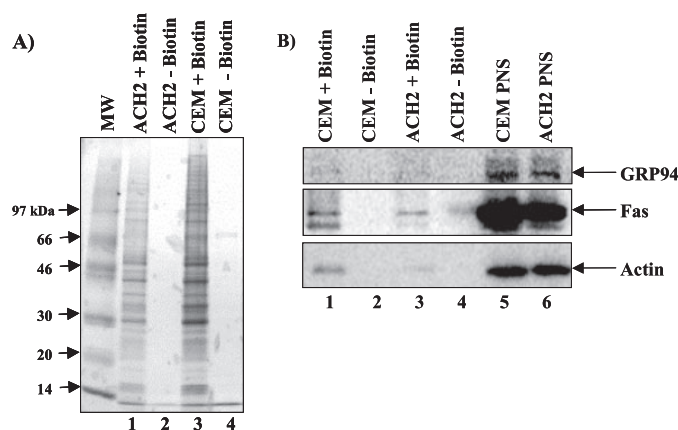


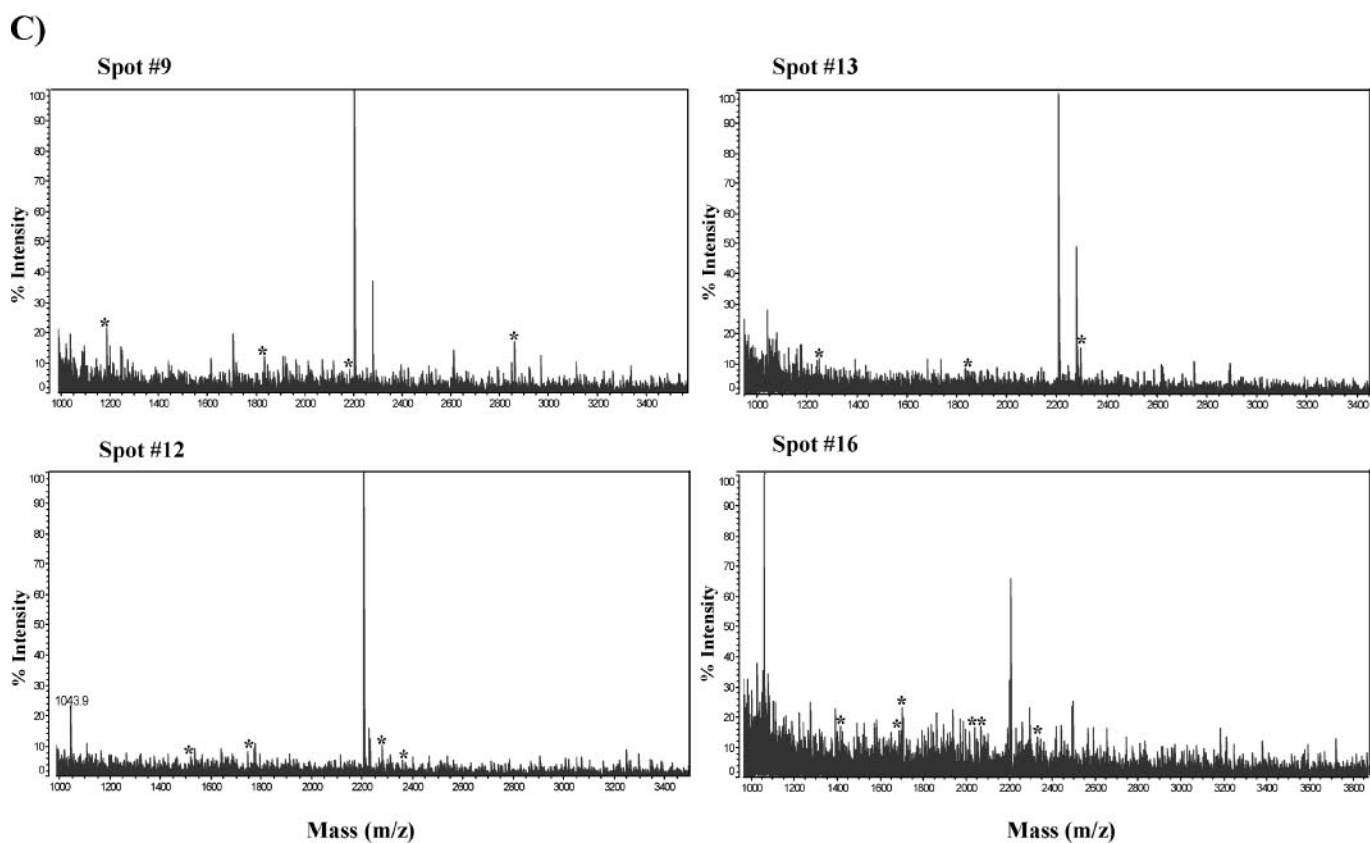
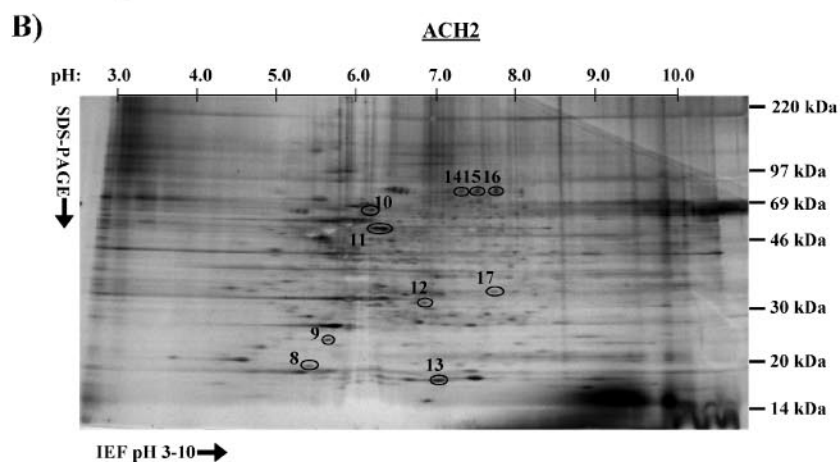
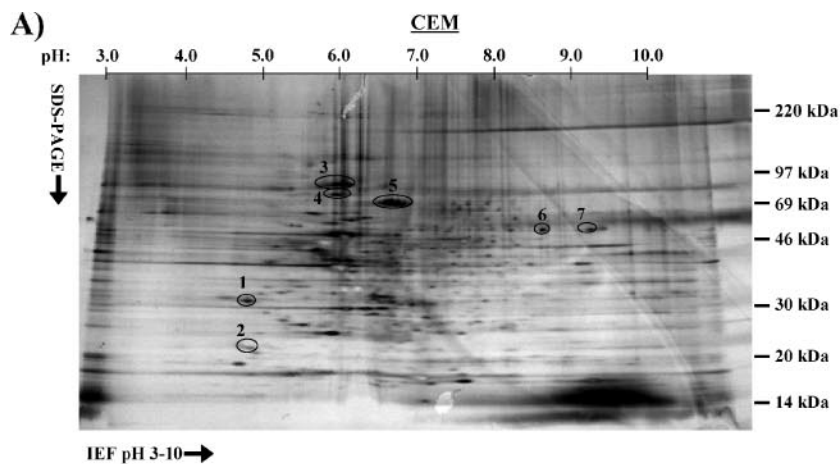
FIGURE 2. **Enrichment for plasma membrane proteins.** A, surface biotinylation and differential centrifugation allows for specific recovery of proteins. PMF proteins were isolated as described in Fig. 1. One-tenth (or 5×10^7 cell eq) of total PMF proteins isolated with and without biotin and 30 μ g of PNS were separated by SDS-PAGE then stained with Coomassie Blue and imaged using Bio-Rad FluorS imager. B, decrease of actin and endoplasmic reticulum-associated GRP94 suggests enrichment for plasma membrane proteins. One-tenth of total PMF proteins and 30 μ g of PNS were separated by SDS-PAGE and blotted with anti-GRP94 and anti-Fas antibodies. The blot was stripped and re-probed with anti-actin antibody. MW, molecular mass standards.

were cut out and further analyzed by trypsin in-gel digestion and MALDI-TOF mass spectrometry, as previously described (19).

MALDI-TOF Analysis

Individual protein spots were excised from the silver-stained two-dimensional gel electrophoresis gel and destained using

Membrane Proteome of HIV-1 Latently Infected Cells



the SilverQuest kit (Invitrogen). Trypsin-digested sample solutions were further desalted and concentrated with C18 ZipTips (Millipore). Samples were mixed with an equal volume of the matrix solution (α -cyano-4-hydroxycinnamic acid in 50% acetonitrile, 0.1% (v/v) trifluoroacetic acid). Two microliters of the mixtures were applied to the sample plate and introduced into the mass spectrometer after drying. Mass spectra were recorded in the reflectron mode of a MALDI-TOF mass spectrometer (Axima CFR Plus, Kratos) operated in delayed extraction mode.

Data Base Analysis

Proteins were identified using the peptide mass fingerprinting analysis software Profound, Prospector, and Mascot. The NCBIInr and SwissProt databases were used for the searches utilizing a maximum of one missed cleavage by trypsin and a mass tolerance of 1 Da. In general, all spots were searched with biotinylation as a variable modification and no-limitation for pI and protein mass. The identified proteins were chosen on the basis of having a low expectation value and also having a molecular weight and pI that is consistent with the values observed on our two-dimensional gel electrophoresis gel, with limitation of the taxonomic category to Homo sapiens.

Flow Cytometry

For cell cycle analysis, cells treated or untreated with drugs were collected by low speed centrifugation and washed with PBS without Ca^{2+} and Mg^{2+} and fixed with 70% ethanol. For fluorescence-activated cell sorting (FACS) analysis, cells were stained with a mixture of propidium iodide (PI) solution (PBS with Ca^{2+} and Mg^{2+} , 10 $\mu\text{g}/\text{ml}$ RNase A, 0.1% Nonidet P-40, and 50 $\mu\text{g}/\text{ml}$ PI) for 30 min at room temperature before analysis. The cells were acquired and analyzed using CELLQuest software (BD Biosciences). Acquired FACS data were analyzed by ModFit LT software (Verity Software House, Inc.).

Fluorescent Staining

HLM-1 or HeLa T4+ cells were grown on glass slides for 6 days in the presence or absence of 2 mM sodium butyrate (NaB). On day 4, cells were transfected with pGFP-BTK, a plasmid that expresses a BTK-GFP fusion protein (16). Two days after transfection (6 days after NaB stimulation), cells were fixed for 1 h in 4% paraformaldehyde (Fisher) at room temperature. Cells were then permeabilized with 0.5% Triton X-100 in PBS for 20 min. Next, cells were washed with PBS without Mg^{2+} and Ca^{2+} . After the wash, cells were incubated with RNase A at 10 $\mu\text{g}/\text{ml}$ for 30 min at 37 °C and washed again with PBS without Mg^{2+} and Ca^{2+} . Cells were incubated with the nuclear stain TOTO-3, a dimeric cyanine nucleic acid stain from Molecular Probes, at 2 μM for 1 h in the dark at 37 °C. Slides were washed with water, and coverslips were mounted using Prolong anti-fade (Molecular Probes).

Confocal Laser Scanning Microscopy

Slides were viewed with a Bio-Rad MRC1024 confocal laser scanning microscope using the 60 \times oil objective and Bio-Rad LaserSharp software Version 5.2. Double excitation at 488 (for detection of GFP) and 647 nm (for DNA stain) was used. Optical sections were taken using z dimensions of 1.0 μm . Pictures were produced using Adobe Photoshop5.0 and Bio-Rad plug-ins.

RESULTS

Surface Protein Biotinylation and Plasma Membrane Protein Isolation—We analyzed the differential expression of surface proteins in T-cells latently infected or uninfected with HIV-1 to identify surface markers for latency and targets for antibody or drug development. Surface proteins were labeled using a biotin-directed affinity purification method described in Fig. 1. In this procedure Sulfo-NHS-Biotin (EZ-Link from Pierce) reacts with ϵ -amines on surface proteins to form a stable complex on intact CEM and ACH2 cells. After surface biotinylation, centrifugation, streptavidin affinity purification, and washing, PMF proteins were isolated, and specific recovery of proteins was determined. No proteins were isolated from cells that were not treated with biotin (Fig. 2A, lanes 2 and 4), demonstrating that the proteins isolated from cells treated with biotin (Fig. 2A, lanes 1 and 3) were specifically pulled down by streptavidin beads. To test for the presence of protein contaminants from other organelles in the PMF, we assayed for GRP94, an endoplasmic reticulum-specific protein. GRP94 was only detected in the PNS of ACH2 and CEM cells but not in the PMFs as determined by Western blot (Fig. 2B, top panel, lanes 1 and 3), suggesting that there is no contaminating organelle proteins in our plasma membrane preparation. On the other hand, the plasma membrane protein Fas was detected in the PMFs of biotin-labeled ACH2 and CEM cells, indicating enrichment of plasma membrane-specific proteins in these fractions (Fig. 2B, middle panel, lanes 1 and 3). Throughout our preparation, high salt and high pH buffers have been employed specifically to abolish non-covalent protein associations and depolymerize actin bundles. Actin levels in PMF were low as compared with PNS (Fig. 2B, bottom panel, lanes 1, 3, 5, and 6), showing that our wash conditions removed most of the actin associated with the membrane fractions. These results suggest that the isolated PMFs are enriched with plasma membrane proteins and have very low or no cytoskeletal proteins or other subcellular compartment contaminants, consistent with previous studies employing surface biotinylation for the isolation of plasma membrane proteins (14, 17).

Identification of Plasma Membrane Proteins Unique to Latent HIV-1 Infection by Two-dimensional Gel Electrophoresis/MALDI-TOF—Membrane fractions isolated from latently infected ACH2 and uninfected CEM cell lines were

FIGURE 3. **Two-dimensional gel electrophoresis analysis of HIV-infected and uninfected plasma membrane proteins.** PMF proteins from CEM cells (A) and ACH2 cells (B) were separated by two-dimensional gel electrophoresis. Gels were stained with mass spectrometry-compatible silver stain. Numbered spots are unique spots for either CEM or ACH2 that were excised and further analyzed by trypsin in-gel digestion and MALDI-TOF mass spectrometry. C, typical MALDI-TOF mass spectra of in-gel-digested sample spots (9, 12, 13, 16) from two-dimensional gel electrophoresis. Star-labeled peaks of each spectrum refer to peptides matched for specific protein candidates found in the data base.

TABLE 1

List of all surface proteins unique to CEM and ACH2 identified by MALDI-TOF analysis

For all the spots (1–17), the identified name, NCBI ID number, computed isoelectric point (pI), molecular weight, percent coverage, and percent of matched peptides are listed.

Spot no.	Name	NCBI ID no.	pI	MW	Coverage %	Peptide matched %
1	Uroplakin Ib (tetraspanin 20)	O75841	5.4	29.7	5	50
2	Protein phosphatase-1 regulatory subunit 7 β 2	AAD26613.1	4.9	27.3	21	34
3	Smooth muscle cell-associated protein 1 (SMAP-1)	BAB20266.1	5.8	101.7	13	40
4	cAMP-specific phosphodiesterase 8A	O60658	5.8	93.3	11	46
5	O-Linked mannose β 1,2-N-acetylglucosaminyltransferase and DNCH1	BAB71960.1	6.4	75.2	26	27
		AAH21297.1	6.7	93.9	21	29
6	Transforming growth factors β receptor I	47937325	8.3	47.7	14	66
7	Phosphorylation regulatory protein HP-10	gi: 627570	9.5	55.1	8	100
8	Melanoma-associated antigen p97, melanotransferrin	NP_201573	5.6	32.7	24	36
9	Bruton's tyrosine kinase	gi: 7157911	5.6	20.5	31	45
10	Interleukin 1 receptor-associated kinase 1b	gi: 14485012	6.2	73.3	12	38
11	X-linked inhibitor of apoptosis	P98170	6.2	56.7	11	44
12	Junctional adhesion molecule 3	Q9B \times 67	7.5	35.0	22	36
13	T cell receptor ER3 β chain	667015	7.9	14.0	32	60
14	M-phase phosphoprotein-1	gi: 2674350	7.7	87.9	7	50
15	Ligatin	P41214	7.6	65.0	12	36
16	γ -Heregulin	gi: 2406644	7.4	84.2	12	75
17	Ornithine transcarbamylase	gi: 360432	8.75	39.9	11	43

TABLE 2

List of matched peptide sequences from spots 9, 12, 13, and 16

For each spot, the measured mass of matched peptide (star-labeled in Fig. 3C), the corresponding computed mass, peptide sequence, residues it spans (start and end), and the number of trypsin-missed cleavage (cut) are indicated.

Spot no.	Measured M_r	Computed M_r	Residues			Matched peptide sequences
			Start	To	Cut	
9	1188.7	1188.6	41	51	0	(R) NCLVNDQGVVK (V)
	1836.9	1835.9	74	88	1	(K) FPVVRWSPPEVLMYSK (F)
	2184.9	2183.9	19	35	1	(K) DVCEAMEYQESKQFLHR (D)
	2853.2	2852.2	8	30	1	(R) FQTQQLLEMCKDVCEAMEYQESK (Q)
12	1551.1	1551.8	176	189	1	(R) NDVPLPTDSRANPR (F)
	1748.4	1747.8	70	83	0	(K) IQDEQTTYVFFDNK (I)
	2280	2279.1	284	303	1	(K) NPGKPDGVNYIRTDEEGDFR (H)
	2361.9	2362.4	15	35	1	(R) LPDFFLLLLFRGCLIGAVNLK (S)
13	1244.5	1244.6	73	80	1	(R) FSPKSPDK (A)
	1835.8	1835.9	19	31	1	(K) YLVTQMGNDKSIK (C)
	2296	2295.2	54	72	1	(K) IMFSYNNKELIINETVPIR (F)
16	1426.2	1425.7	34	46	1	(K) APQKSYSSSETLK (A)
	1691.7	1692.0	321	335	1	(R) STFARPAFNLKPKSK (Y)
	1700.9	1700.8	626	640	1	(R) INKASLADSGEYMCK (V)
	2039.4	2040.0	626	640	1	(R) INKASLADSGEYMCK (V)
	2070.2	2071.2	549	567	1	(K) ESEVVSFLTATAIALPRLK (E)
	2346.2	2346.1	715	734	1	(K) TFCVNGGECFMVKDLSNPSR (Y)

separated by two-dimensional gel electrophoresis and silver-stained. Unique proteins from both cell lines (spots 1–17, Fig. 3A and B) were excised, in-gel-digested with trypsin, eluted from the gel, and identified by MALDI-TOF as previously described (19). Data base searches (NCBI nonredundant and SWISS-PROT) point to 17 candidate proteins listed in Table 1. Fig. 3C shows examples of peptide mass fingerprint spectra generated by MALDI-TOF after analysis of four different spots. Starred peaks refer to peptides matched for specific protein candidates found in the data base. Peptide sequences of the four selected spots in Fig. 3C are listed in Table 2, and the peptide sequences of all 17 spots are listed in supplemental Table 1. Interestingly, 47% of the identified proteins are integral membrane proteins, 18% are membrane-associated, 29% are cytoplasmic, many of which are associated with the cytoskeleton, and 6% are associated with the Golgi apparatus.

HIV-1 Regulates Apoptosis through Up-regulation of XIAP—The anti-apoptotic protein X-linked inhibitor-of-apoptosis (XIAP) was identified as one of the proteins up-regulated in the membrane fractions of the latently infected ACH2 cell line. To

confirm this result, we performed a Western blot analysis and showed that XIAP was more enriched in the membrane fraction isolated from biotin-labeled ACH2 than CEM cells (Fig. 4A, lanes 2 and 4). Fractions isolated from ACH2 and CEM without biotinylation were used as a negative control and did not show any binding to XIAP (Fig. 4A, lanes 1 and 3). To test whether the increased XIAP levels in the ACH2 membrane fractions was due to HIV-1 induced translocation of the protein to the membrane or to an overall increase in XIAP levels in the cell, we performed a Western blot on ACH2 and CEM whole cell extracts and found that XIAP levels were generally higher in latently infected cells (Fig. 4B). XIAP levels were also observed to be higher in other HIV-latently infected cells including J1-1 and OM10.1 as compared with the uninfected cells Jurkat and THP-1 (Fig. 4C). Interestingly when we compared XIAP levels in the uninfected U937 and HIV latently infected U1 monocytes, we observed a prominent 30-kDa cleaved XIAP form in the uninfected cells but not the infected cells (Fig. 4C). It has been shown that the cleaved form of XIAP has a significantly reduced potency compared with the full-length XIAP (20). Our

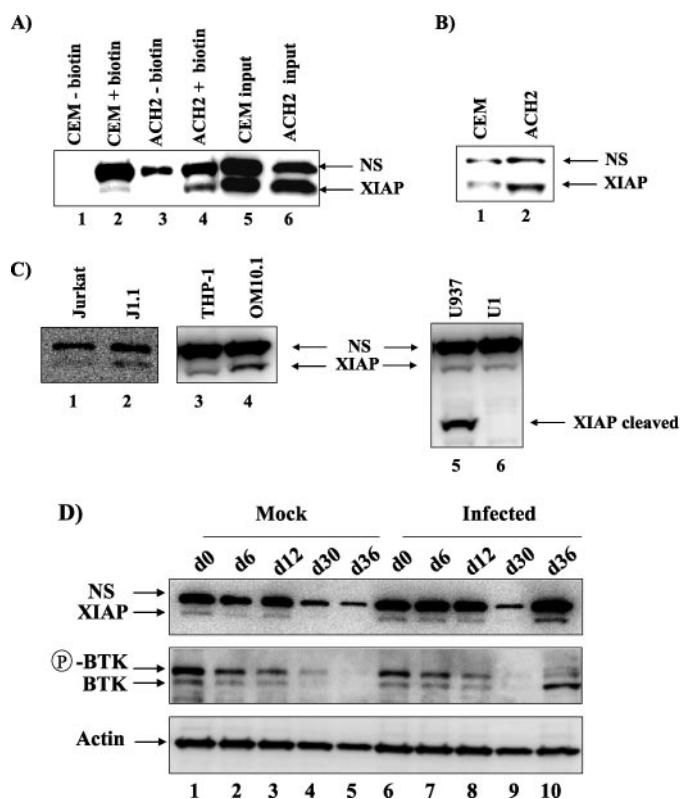


FIGURE 4. XIAP up-regulation in ACH2 cells and latently infected PBMC. A, ACH2 and CEM PMF proteins from Fig. 2 were separated by SDS-PAGE blotted with anti-XIAP antibody. ACH2 and CEM (B) and Jurkat, J1-1, THP-1, OM10.1, U937, and U1 whole cells (5×10^4) (C) were solubilized in Laemmli buffer, run on SDS-PAGE, and blotted with anti-XIAP antibody. D, levels of XIAP, BTK, and actin at different time points after infection or mock infection of PBMC by Western blot. NS refers to a nonspecific band. P-BTK refers to phosphorylated BTK, and BTK refers to the unphosphorylated form.

results demonstrate that the full-length active form of XIAP is found in infected monocytes (U1), whereas the less active cleaved form is found in uninfected monocytes (U937), further proving the differential regulation of XIAP as a result of latent infection albeit through a different mechanism in monocytes. After observing that XIAP is up-regulated in latently infected cell lines, we wanted to determine whether a similar result will be obtained during latent infection of primary T-lymphocytes. Therefore, we infected PBMC with HIV-1 provirus at 1000 TCID₅₀. Cells were analyzed for levels of XIAP at different time points during acute infection (days 6 and 12), and later phases of infection (days 30 and 36) were characterized by low levels of virus replication as a result of viral latency (21). During acute infection at 6 and 12 days, we observed a constant level of XIAP in infected as well as mock-infected cells. At day 30, XIAP levels decreased dramatically both in mock and infected cells, indicating a dramatic decrease in cell viability. However, at day 36, a significant increase in XIAP levels was observed in infected cells in the surviving population but not in the mock-infected cells (Fig. 4D). This surviving population has been previously shown to contain the latent virus (21).

Inhibition of XIAP Expression with Flavopiridol Sensitizes Latently Infected ACH2 Cells to Apoptosis—After showing that XIAP is up-regulated in latently infected cells, we wanted to determine whether inhibiting XIAP expression might sensitize

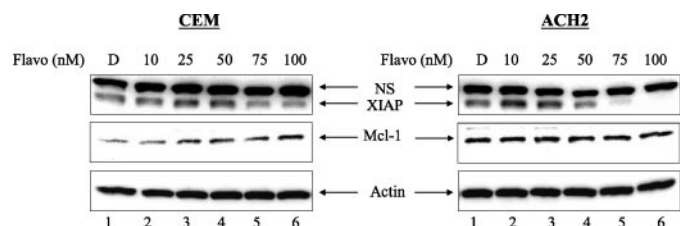


FIGURE 5. Flavopiridol inhibits XIAP protein levels. ACH2 and CEM cells treated with different concentrations of flavopiridol (10, 25, 50, 75, and 100 nM) were solubilized in Laemmli buffer and blotted with anti-XIAP, anti-Mcl-1, and anti-actin as a control. D refers to Me₂SO treatment as a control.

infected cells to cell death. Flavopiridol is a cyclin-dependent kinase inhibitor that has also been shown to specifically down-regulate expression of XIAP and sensitizes cells to apoptosis (22–24). Flavopiridol treatment slightly decreased XIAP expression in CEM cells but resulted in a more dramatic decrease in XIAP levels in ACH2 cells. Treatment with 100 nM flavopiridol resulted in a complete loss of XIAP expression in ACH2 but not in CEM cells (Fig. 5). Another anti-apoptotic protein Mcl-1 was differentially regulated in CEM and ACH2 cells. Mcl-1 increased as a response to flavopiridol treatment in CEM cells but decreased in ACH2 cells (Fig. 5, middle panels). The Mcl-1/actin ratio doubled in CEM cells treated with 100 nM flavopiridol as compared with untreated cells but decreased by half in ACH2 after treatment with 100 nM flavopiridol. Interestingly, the overall level of Mcl-1 in infected cells (ACH2) was higher than in uninfected cells (CEM), further indicating that anti-apoptotic proteins are up-regulated in latently infected cells. The effect of flavopiridol on cell death was assessed by determining PARP cleavage, caspase-3 activation, and the level of apoptosis by flow cytometry. Treatment of ACH2 and CEM cells with flavopiridol resulted in a dose-dependent increase in PARP cleavage (Fig. 6A). At high concentrations of flavopiridol (75 and 100 nM), complete cleavage of PARP was induced in ACH2 but not in CEM cells (Fig. 6A, top panel, lanes 5, 6, 11, and 12). Because XIAP is known to mediate its anti-apoptotic activity by blocking caspase-3 cleavage, we analyzed the effect of flavopiridol on caspase-3 cleavage in ACH2 and CEM cells. Although pro-caspase-3 levels did not change in CEM-treated cells, it was cleaved in a dose-dependent manner in flavopiridol-treated ACH2 cells (Fig. 6A, middle panel). Actin levels did not change upon flavopiridol treatment (Fig. 6A, bottom panel). Finally, we performed FACS to determine the level of apoptosis in ACH2, CEM, and A3.01 cells. A3.01 is a hypoxanthine/aminopterin/thymidine (HAT)-sensitive derivative of CEM from which ACH2 cells were directly derived. In mock-treated cells, the levels of apoptosis were low in all three cell lines (Fig. 6B), whereas treatment with 100 nM flavopiridol dramatically increased the level of apoptosis in ACH2 cells (58.3%) but not significantly in CEM and A3.01 cells (Fig. 6B). Taken together, these results indicate that HIV-1-infected cells are more sensitive to flavopiridol-induced apoptosis.

HIV-1 Regulates Receptor Signaling by Inducing Translocation of BTK to the Plasma Membrane—According to our data base analysis, BTK was identified as one of the proteins that is enriched in the ACH2 membrane fractions as compared with CEM. Although BTK expression was similar in ACH2 and CEM cells as determined by Western blot in Fig. 7A, the phosphoryl-

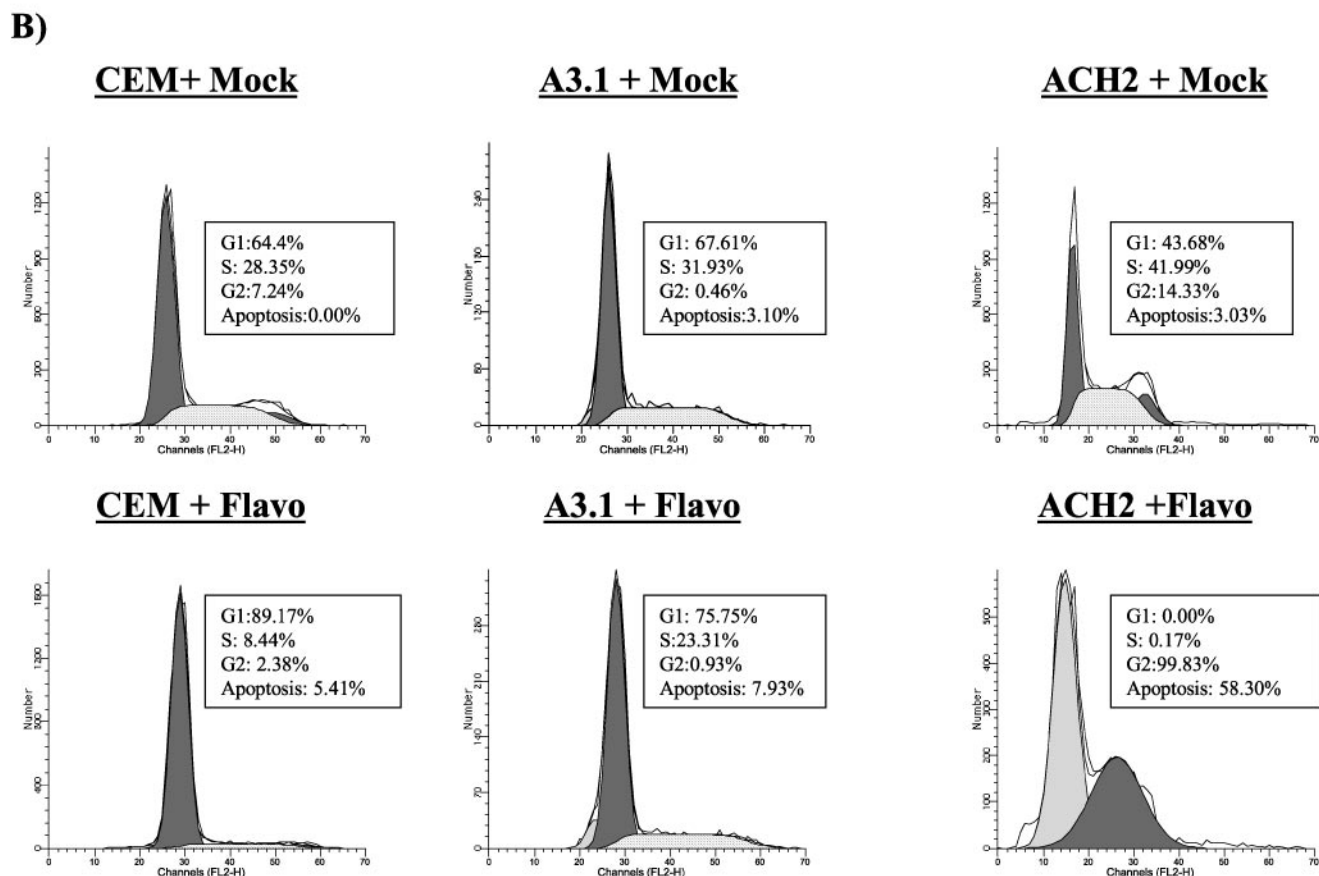
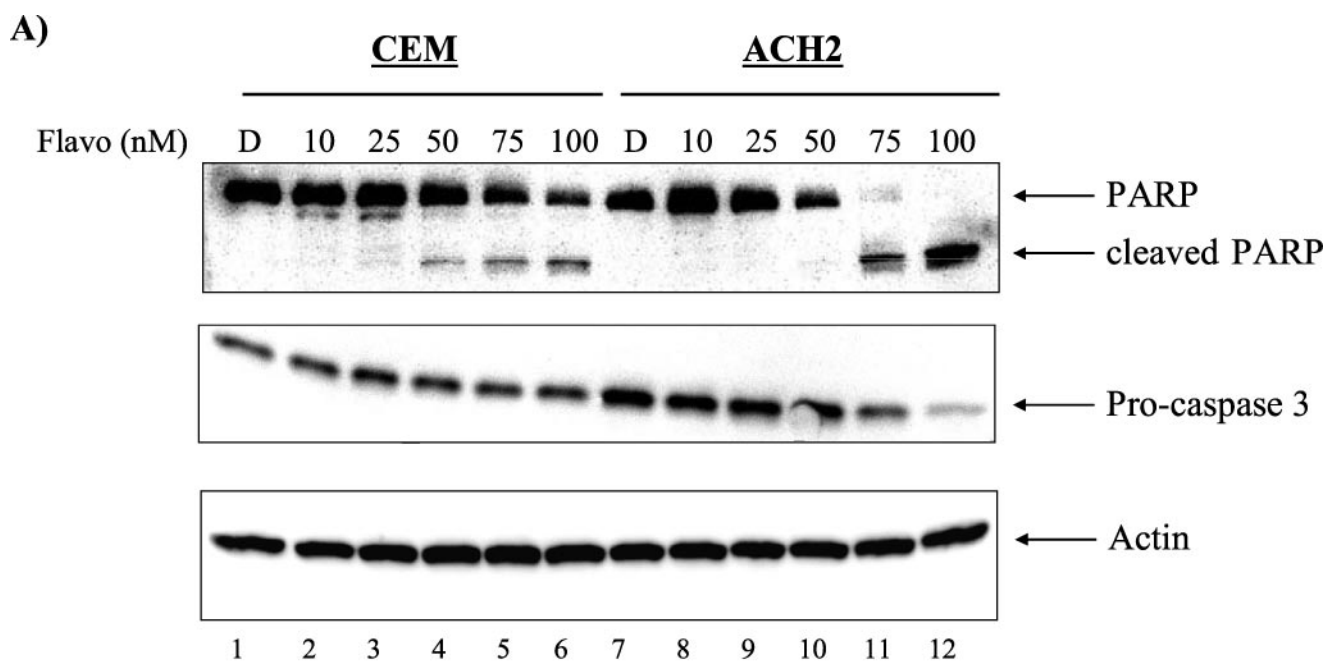


FIGURE 6. **Flavopiridol induces apoptosis in HIV-1-infected cells.** A, ACH2 and CEM cells treated with different concentrations of flavopiridol (10, 25, 50, 75, and 100 nM) were solubilized in Laemmli buffer and blotted with anti-PARP, anti-caspase-3, and anti-actin antibodies. B, FACS analysis of mock-treated cells and cells treated with 100 nM flavopiridol. CEM, A3.01, and ACH2 cells were stained with a mixture of phosphatidylinositol buffer followed by cell sorting analysis. Acquired FACS data were analyzed by ModFit LT software. This figure is a representative experiment of three independent experiments with very similar results.

ated form of the protein was significantly increased in ACH2 cells. In addition, other infected cells such as J1-1 and OM10.1 had a higher level of BTK as compared with uninfected Jurkat

and THP-1 cells (Fig. 7A). Although J1-1 showed higher levels of both forms of BTK as compared with Jurkat, phosphorylated BTK was significantly up-regulated in OM10.1 cells as com-

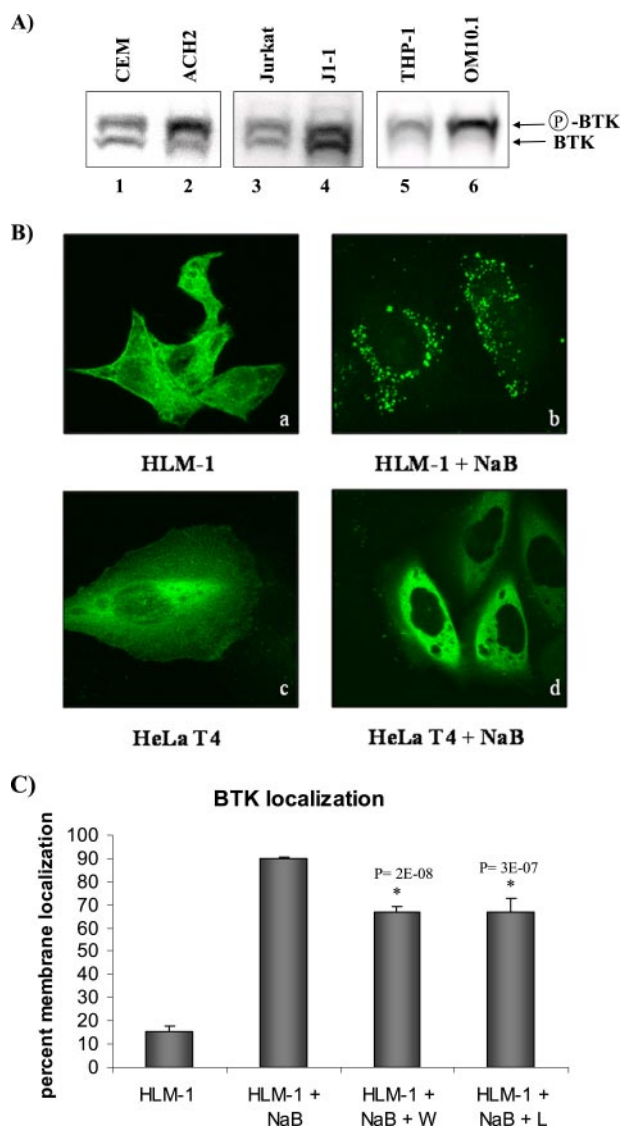


FIGURE 7. BTK plasma membrane localization in infected cells. *A*, CEM, ACH2, Jurkat, J1-1, THP-1, and OM101.1 whole cells (5×10^4) were solubilized in Laemmli buffer and blotted with anti-BTK antibody. *B*, HLM-1 cells were treated with 2 mM NaB and transfected with the pGFP-BTK plasmid on day 4. On day 6, cells were fixed, permeabilized, and stained for DNA using TOTO-3. Cells were examined for the localization of the GFP-BTK fusion protein (green). Panels *a–d* represent a projection of series of 1- μ m sections through HLM-1 cells (panel *a*), HLM-1 cells treated with NaB (panel *b*), untreated HeLa-T4+ cells (panel *c*), and HeLa-T4+ treated with NaB (panel *d*). *C*, effect of PI3K inhibitors on BTK localization. HLM-1 cells were treated with the PI3K inhibitors wortmannin (W) and LY294002 (L) for 15 min after NaB stimulation and GFP-BTK transfection. BTK localization was determined by confocal microscopy as in *B*, and the percent of BTK localized at the plasma membrane is illustrated in the graph. *p* values were obtained from three independent experiments.

pared with THP-1. We hypothesized that the increase in BTK observed in the ACH2 membrane fractions could be due to the increased translocation of BTK to the membrane where it becomes phosphorylated. We transfected HLM-1 cells with GFP-BTK and monitored localization of the protein by fluorescent confocal microscopy before and after stimulation with sodium butyrate (NaB) to activate the virus. BTK was predominantly localized in the cytoplasm before induction of HLM-1 (Fig. 7*B*, panel *a*). However, after NaB treatment, the distribu-

tion of GFP-BTK was altered, and BTK was concentrated into patches on the surface of the cells (Fig. 7*B*, panel *b*). This redistribution of BTK to the cell surface is specific to virus activation since treatment of HeLa-T4+ with NaB did not result in translocation of BTK to the plasma membrane (Fig. 7*B*, panels *c* and *d*). BTK translocation to the plasma membrane is phosphatidylinositol 3-kinase (PI3K)-dependent and is inhibited by the PI3K inhibitors wortmannin and LY294002 (25). Therefore, we treated HLM-1 cells with these two inhibitors separately and asked whether treatment with these agents would reverse virus-induced BTK translocation to the plasma membrane. Results in Fig. 7*C* indicated that BTK was localized to the plasma membrane in around 90% of HLM-1 cells treated with NaB. After treatment with wortmannin and LY294002 for 15 min, the percentage of membrane-associated BTK decreased 25%, indicating that translocation of BTK may be regulated by PI3K. Using the same latent infection of primary cell system described in Fig. 4*D*, we determined BTK levels during acute and latent infection. Both phosphorylated and unphosphorylated forms of BTK decreased during acute infection on days 6 and 12 (Fig. 4*D*, middle panel). On day 30, BTK expression was lost in both mock- and HIV-1-infected cells, indicating a decrease in cell viability. However, at day 36 we observed a significant increase in both forms of BTK in the surviving population of infected cells but not in mock-infected cells, indicating that this increase is the result of latency.

DISCUSSION

In this study we applied a recently developed method for the isolation of plasma membrane-associated proteins based on the use of biotin to label surface proteins. This biotin-affinity method has several advantages over more traditional approaches (*i.e.* density gradients using ultracentrifugation and sucrose/Percoll, lectin affinity enrichment combined with centrifugation, and silica beads) to isolate plasma membrane proteins, including the significant reduction in contamination by mitochondrial/endoplasmic reticulum membrane proteins, higher yield of plasma membrane proteins, higher reproducibility, and less preparation time. We demonstrated the specificity of this method by showing that streptavidin beads specifically precipitate the biotinylated membrane fraction as shown in Fig. 2*A*. In addition, unlike more traditional membrane isolation methods, there was very little to no organelle or cytoskeletal protein contaminants detected after plasma membrane enrichment by biotin-affinity membrane purification (Fig. 2*B*). An added advantage is that biotinylation of the plasma membrane proteins has been shown not to interfere with membrane receptor activity or signal transmission. Thus, affinity enrichment utilizing biotinylation/streptavidin capture provides efficient isolation of membrane proteins without altering the biomembrane landscape (14, 26).

We employed the biotin-based affinity method to compare the membrane proteome of latently infected HIV-1 cells (ACH2) to uninfected cells (CEM) and identify membrane-associated latency markers that can be targeted by drugs or antibodies. In latently infected cells, viral expression is down-modulated, leaving the provirus in a latent state characterized by low or absent viral mRNA and protein production (27, 28).

Membrane Proteome of HIV-1 Latently Infected Cells

Under basal transcription conditions, the latently infected ACH2 cells produce predominantly multiply spliced transcripts encoding HIV-1 regulatory proteins including Tat, Nef, and Vpr but are unable to produce a significant amount of virus (13).

We identified 17 differentially expressed proteins in ACH2 cells by MALDI-TOF. The majority of the identified proteins (65%) are integral membrane or membrane-associated proteins that can be divided into two functional categories. The first is cell adhesion, structure, and migration and contains uroplakin 1b (tetraspanin 20), p97 isoform 2, junction adhesion molecule 3, and ligatin. The second category represents receptors or receptor-associated proteins involved in the regulation of cell death and survival and includes transforming growth factor beta-receptor I, T-cell receptor ER3 β chain, γ -heregulin, interleukin-1 receptor kinase 1b, BTK, and XIAP. It is not known how HIV causes changes in cellular phenotype before the transition into latency. It is possible that infection induces a change in cellular physiology that is not reversed when the infected cell enters a quiescent or latent state. On the other hand, it is possible that HIV-1 regulatory proteins produced from multiply spliced transcripts as a result of basal transcription in latently infected cells might alter several pathways to enhance the homing, spreading, and survival of infected lymphocytes, thus contributing to the establishment and maintenance of viral latency.

HIV-1 Infection Ensures a Balance between Cell Survival and Apoptosis—HIV-1-induced apoptosis plays an important role in the pathogenesis of AIDS. Several viral proteins contribute to the induction of apoptosis including Vpr, Vpu, and Tat (29–32). Although a growing body of evidence suggests that the HIV-1 accessory proteins, namely Nef and Vpr, could be involved in depletion of CD4⁺ and non-CD4⁺ cells and in tissue atrophy, they also have been implicated in delaying the death of HIV-1-infected cells (33). These apparently contradictory observations can be explained by the fact that cell depletion is likely to be predominantly a bystander effect by extracellular or cell surface-associated components of HIV-infected cells (34, 35).

This study provides evidence that XIAP increases in latently infected cell lines (Fig. 4). In addition, Li *et al.* (21) have demonstrated that the gradual loss of HIV expression in chronically infected cells a few weeks after infection was not due to dying out of infected cells nor overgrowth of uninfected cells but was due to gradual cessation of HIV production in the vast majority of the productively infected cells. Based on these results and other similar studies, we monitored XIAP levels in infected PBMC over a period of 36 days and observed an increase in XIAP level in a surviving population that has previously been shown to be latently infected (Fig. 4D). We believe that up-regulation of anti-apoptotic proteins stems from the dependence of latently infected cells on mechanisms to increase cell survival as a way to counterbalance the apoptotic effects of some viral accessory proteins.

XIAP suppresses apoptosis by inhibiting the protease activity of caspases 3, 7, and 9 (36). XIAP expression can be inhibited by flavopiridol, a cyclin-dependent kinase inhibitor that has varying activities against multiple cyclin-dependent kinase (CDK) family members but has the highest potency against CDK9 (22,

37, 38). A genome-wide analysis using DNA microarrays has shown that flavopiridol inhibits transcription globally in a manner highly similar to the transcription inhibitors actinomycin D and 5,6-dichloro-1- β -D-ribobenzimidazole (DRB), predominantly through its ability to inhibit P-TEFb (39). This same study demonstrated that flavopiridol inhibited mostly genes with short mRNA half-lives including M-phase regulators and anti-apoptotic proteins such as the three members of the inhibitor of apoptosis family (c-IAP1, cIAP2, and NIAP). Other reports have shown that flavopiridol induces down-regulation of XIAP at the transcriptional level and sensitizes cells to apoptosis (22–24). We provided evidence that latently infected cells were more sensitive to flavopiridol-induced apoptosis than uninfected cells. In fact, flavopiridol treatment resulted in a dramatic decrease in XIAP protein levels, complete PARP cleavage, caspase-3 activation, and an increase in apoptosis in ACH2 cells but not in uninfected CEM cells (Figs. 5 and 6). The higher sensitivity of ACH2 cells to flavopiridol is likely due to the dependence of the infected cells on cyclin-dependent kinase 9, the main target of flavopiridol (40). It is possible that certain viral proteins, namely Tat, increase the sensitivity of infected cells to flavopiridol since it has been shown that the presence of Tat renders cyclin-dependent kinase 9 activity more sensitive to flavopiridol inhibition (41). Another cell cycle feature for latently infected cells treated with flavopiridol is the G₁ block observed in CEM cells but not in ACH2 cells (Fig. 6B). Flavopiridol, at concentrations within the ranges used in our experiment, was reported to induce p21/Waf1, leading to a G₁ block (42). We have previously published that although CEM cells express a high level of p21/Waf1, ACH2 cells lose their G₁/S checkpoint due to the lack of p21/Waf1 (13). It seems that uninfected CEM cells are able to overcome this block at G₁/S, allowing time to repair and detoxify before S-phase entry and maintaining a low level of apoptosis. On the other hand, the loss of G₁ block in ACH2 cells could explain the high cell death in these cells as a response to flavopiridol treatment (Fig. 6B).

Another protein affected by flavopiridol treatment was Mcl-1. Mcl-1 is an anti-apoptotic protein that has been shown to decrease in response to flavopiridol treatment in leukemia cells and other types of cancer cells (43). In addition, it was reported that Mcl-1 increases in AIDS-related malignancies (44, 45). Consistent with these observations, our results demonstrate that the overall level of Mcl-1 is higher in infected cells (ACH2) than in uninfected cells (CEM) (Fig. 5). The increase of Mcl-1 in CEM as a result of flavopiridol treatment (Fig. 5) helps explain the resistance of CEM to flavopiridol-induced cell death (Fig. 6B). On the other hand, the decrease in Mcl-1 in ACH2 cells after treatment with flavopiridol possibly contributes to the sensitivity of ACH2 cells to death induced by flavopiridol. This evidence contributes further to our hypothesis that latently infected cells are more dependent on survival factors such as XIAP and Mcl-1 as compared with uninfected cells. Therefore, targeting these survival proteins with drugs renders infected cells more prone to cell death than uninfected cells.

HIV-1 Latency Regulates Cell Signaling—BTK was also found to be up-regulated on the surface of latently infected cells. BTK is a member of the Tec family of protein-tyrosine kinases, which in turn belongs to the Src superfamily (46). BTK is

involved in B-cell receptor signaling and, thus, directs B-cell lineage development. PI3K activation leads to membrane translocation of BTK via its association with the phosphoinositide, phosphatidylinositol 3,4,5-trisphosphate, which associates with the pleckstrin homology domain of BTK (16, 47). BTK has a dual role in apoptosis and cell survival. Although it promotes apoptosis in HeLa cells, it has a protective effect against apoptosis in B cells. In fact, BTK-mediated survival may depend on the PI3K pathway or on the BTK activation of members of the anti-apoptotic machinery (48). It is also believed that BTK mediates survival signals through the NF κ B pathway (49). According to our results, HIV infection affects the translocation of BTK to the plasma membrane (Fig. 7). In fact, we showed that BTK localizes in the cytoplasm of HLM-1 cells before stimulation of the virus, whereas it translocates to the membrane into distinct patches after virus activation (Fig. 7B). These results indicate that the translocation of BTK was virus-dependent and may suggest the localization of BTK to specialized patches on the cell surface or lipid rafts known to be important sites for virus budding (50). A recent study has shown that PI3K-dependent translocation of BTK to the plasma membrane is inhibited by the PI3K inhibitors wortmannin and LY294002 (25). After treatment of NaB-stimulated HLM-1 with wortmannin and LY294002, localization of BTK to the membrane decreased significantly as compared with stimulated HLM-1 in the absence of inhibitors (Fig. 7C). These results show that translocation of BTK to the membrane in infected cells may be mediated by PI3K, which was previously shown to be needed for HIV-1 replication (51). This suggests that blocking PI3K-dependent BTK translocation to the membrane may inhibit HIV-1 infection.

In conclusion, we believe that identifying the membrane proteome of infected cells reflects changes that happen on the cell surface due to viral pathogenesis and may allow us to determine pathways that are important for the maintenance of latency. Targeting several pathways that are altered in infected cells will help define new therapies to eradicate latently infected cells that cannot be targeted by highly active anti-retroviral therapy treatment.

Acknowledgments—HLM-1, Hel-T4+, CEM, A3.01, and ACH2 were obtained from the National Institutes of Health AIDS reagent program. We thank Edvard Smith, Huddinge University Hospital, Sweden for the BTK-GFP plasmid.

REFERENCES

- Singer, S. J., and Nicolson, G. L. (1972) *Science* **175**, 720–731
- Brown, D. A., and London, E. (2000) *J. Biol. Chem.* **275**, 17221–17224
- Dietrich, C., Bagatolli, L. A., Volovyk, Z. N., Thompson, N. L., Levi, M., Jacobson, K., and Gratton, E. (2001) *Biophys. J.* **80**, 1417–1428
- Jacobson, K., and Dietrich, C. (1999) *Trends Cell Biol.* **9**, 87–91
- Friedrichson, T., and Kurzchalia, T. V. (1998) *Nature* **394**, 802–805
- Simons, K., and Ehehalt, R. (2002) *J. Clin. Investig.* **110**, 597–603
- Harder, T., and Simons, K. (1997) *Curr. Opin. Cell Biol.* **9**, 534–542
- Chun, T. W., and Fauci, A. S. (1999) *Proc. Natl. Acad. Sci. U. S. A.* **96**, 10958–10961
- Pocernich, C. B., Boyd-Kimball, D., Poon, H. F., Thongboonkerd, V., Lynn, B. C., Klein, J. B., Calebrese, V., Nath, A., and Butterfield, D. A. (2005) *Brain Res. Mol. Brain Res.* **133**, 307–316
- Fuchigami, T., Misumi, S., Takamune, N., Takahashi, I., Takama, M., and Shoji, S. (2002) *Biochem. Biophys. Res. Commun.* **293**, 1107–1113
- Carlson, K. A., Ciborowski, P., Schellpeper, C. N., Biskup, T. M., Shen, R. F., Luo, X., Destache, C. J., and Gendelman, H. E. (2004) *J. Neuroimmunol.* **147**, 35–42
- Ross, E. K., Buckler-White, A. J., Rabson, A. B., Englund, G., and Martin, M. A. (1991) *J. Virol.* **65**, 4350–4358
- Clark, E., Santiago, F., Deng, L., Chong, S., de La Fuente, C., Wang, L., Fu, P., Stein, D., Denny, T., Lanka, V., Mozafari, F., Okamoto, T., and Kashanchi, F. (2000) *J. Virol.* **74**, 5040–5052
- Zhao, Y., Zhang, W., and Kho, Y. (2004) *Anal. Chem.* **76**, 1817–1823
- Berro, R., Kehn, K., de la Fuente, C., Pumfery, A., Adair, R., Wade, J., Colberg-Poley, A. M., Hiscott, J., and Kashanchi, F. (2006) *J. Virol.* **80**, 3189–3204
- Nore, B. F., Vargas, L., Mohamed, A. J., Branden, L. J., Backesjo, C. M., Islam, T. C., Mattsson, P. T., Hultenby, K., Christensson, B., and Smith, C. I. (2000) *Eur. J. Immunol.* **30**, 145–154
- Peirce, M. J., Wait, R., Begum, S., Saklatvala, J., and Cope, A. P. (2004) *Mol. Cell. Proteomics* **3**, 56–65
- Wang, D., de la Fuente, C., Deng, L., Wang, L., Zilberman, I., Eadie, C., Healey, M., Stein, D., Denny, T., Harrison, L. E., Meijer, L., and Kashanchi, F. (2001) *J. Virol.* **75**, 7266–7279
- Wu, K., Bottazzi, M. E., de La Fuente, C., Deng, L., Gitlin, S. D., Maddukuri, A., Li, H., Vertes, A., Pumfery, A., and Kashanchi, F. (2004) *J. Biol. Chem.* **279**, 495–508
- Deveraux, Q. L., Leo, E., Stennicke, H. R., Welsh, K., Salvesen, G. S., and Reed, J. C. (1999) *EMBO J.* **18**, 5242–5251
- Li, X. D., Moore, B., and Cloyd, M. W. (1996) *Virology* **225**, 196–212
- Rosato, R. R., Dai, Y., Almenara, J. A., Maggio, S. C., and Grant, S. (2004) *Leukemia* **18**, 1780–1788
- Dai, Y., Rahmani, M., and Grant, S. (2003) *Oncogene* **22**, 7108–7122
- Wittmann, S., Bali, P., Donapaty, S., Nimmanapalli, R., Guo, F., Yamaguchi, H., Huang, M., Jove, R., Wang, H. G., and Bhalla, K. (2003) *Cancer Res.* **63**, 93–99
- Bober, R., Wilde, J. I., Maschberger, P., Venkateswarlu, K., Cullen, P. J., Siess, W., and Watson, S. P. (2001) *Blood* **97**, 678–684
- Zhang, W., Zhou, G., Zhao, Y., and White, M. A. (2003) *Electrophoresis* **24**, 2855–2863
- Butera, S. T., Roberts, B. D., Lam, L., Hodge, T., and Folks, T. M. (1994) *J. Virol.* **68**, 2726–2730
- Pomerantz, R. J., Trono, D., Feinberg, M. B., and Baltimore, D. (1990) *Cell* **61**, 1271–1276
- Kekow, J., Wachsman, W., McCutchan, J. A., Cronin, M., Carson, D. A., and Lotz, M. (1990) *Proc. Natl. Acad. Sci. U. S. A.* **87**, 8321–8325
- Yang, Y., Tikhonov, I., Ruckwardt, T. J., Djavani, M., Zapata, J. C., Pauza, C. D., and Salvato, M. S. (2003) *J. Virol.* **77**, 6700–6708
- Akari, H., Bour, S., Kao, S., Adachi, A., and Strebel, K. (2001) *J. Exp. Med.* **194**, 1299–1311
- Jacotot, E., Ferri, K. F., El Hamel, C., Brenner, C., Druillennec, S., Hoebeke, J., Rustin, P., Metivier, D., Lenoir, C., Geuskens, M., Vieira, H. L., Loeffler, M., Belzacq, A. S., Briand, J. P., Zamzami, N., Edelman, L., Xie, Z. H., Reed, J. C., Roques, B. P., and Kroemer, G. (2001) *J. Exp. Med.* **193**, 509–519
- Ross, T. M. (2001) *Leukemia* **15**, 332–341
- Finkel, T. H., Tudor-Williams, G., Banda, N. K., Cotton, M. F., Curiel, T., Monks, C., Baba, T. W., Ruprecht, R. M., and Kupfer, A. (1995) *Nat. Med.* **1**, 129–134
- Anderson, R. W., Ascher, M. S., and Sheppard, H. W. (1998) *J. Acquired Immune Defic. Syndr. Hum. Retrovirol.* **17**, 245–252
- Eckelman, B. P., Salvesen, G. S., and Scott, F. L. (2006) *EMBO Rep.* **7**, 988–994
- Carlson, B., Pearlstein, R., Naik, R., Sedlacek, H., Sausville, E., and Worland, P. (1996) *Proc. Am. Assoc. Cancer Res.* **37**, 424 (abstr.)
- Shapiro, G. I. (2004) *Clin. Cancer Res.* **10**, 4270S–4275S
- Lam, L. T., Pickeral, O. K., Peng, A. C., Rosenwald, A., Hurt, E. M., Giltman, J. M., Averett, L. M., Zhao, H., Davis, R. E., Sathyamoorthy, M., Wahl, L. M., Harris, E. D., Mikovits, J. A., Monks, A. P., Hollingshead, M. G., Sausville, E. A., and Staudt, L. M. (2001) *Genome Biology* **2**, RESEARCH0041

Membrane Proteome of HIV-1 Latently Infected Cells

40. Chao, S. H., and Price, D. H. (2001) *J. Biol. Chem.* **276**, 31793–31799
41. Zhou, M., Deng, L., Lacoste, V., Park, H. U., Pumfery, A., Kashanchi, F., Brady, J. N., and Kumar, A. (2004) *J. Virol.* **78**, 13522–13533
42. Blagosklonny, M. V., Darzynkiewicz, Z., and Figg, W. D. (2002) *Cancer Biol. Ther.* **1**, 420–425
43. Chen, R., Keating, M. J., Gandhi, V., and Plunkett, W. (2005) *Blood* **106**, 2513–2519
44. Schlaifer, D., Krajewski, S., Galoin, S., Rigal-Huguet, F., Laurent, G., Massip, P., Pris, J., Delsol, G., Reed, J. C., and Brousset, P. (1996) *Am. J. Pathol.* **149**, 177–185
45. Fernandez-Figueras, M. T., Puig, L., Fernandez-Vasalo, A., Esquiús, M., Montero, M. A., and Ariza, A. (2000) *Mod. Pathol.* **13**, 438–445
46. Mano, H. (1999) *Cytokine Growth Factor Rev.* **10**, 267–280
47. Varnai, P., Rother, K. I., and Balla, T. (1999) *J. Biol. Chem.* **274**, 10983–10989
48. Islam, T. C., and Smith, C. I. (2000) *Immunol. Rev.* **178**, 49–63
49. Petro, J. B., Rahman, S. M., Ballard, D. W., and Khan, W. N. (2000) *J. Exp. Med.* **191**, 1745–1754
50. Nguyen, D. H., and Hildreth, J. E. (2000) *J. Virol.* **74**, 3264–3272
51. Francois, F., and Klotman, M. E. (2003) *J. Virol.* **77**, 2539–2549

